Spectroscopic characterization of *trans–gauche* isomerization in liquid crystal polymers with two nematic states

Regan L. Silvestri and Jack L. Koenig*
Department of Macromolecular Science, Case Western Reserve University, Cleveland, Ohio 44106, USA
(Received 23 August 1993; revised 22 October 1993)

Nuclear magnetic resonance (n.m.r.) spectroscopy and Fourier transform infra-red (*FT*i.r.) spectroscopy are used to characterize the *trans–gauche* isomerization of the methylene groups in a new class of main-chain liquid crystal polymers. This new series of liquid crystalline copolymers is based on the 1-(4-hydroxyphenyl)-2-(2-R-4-hydroxyphenyl)ethane mesogen, where R is F, Cl or CH_3 and flexible spacers containing an odd number of menthylene units. These copolymers are particularly interesting because they show two nematic states. *Trans–gauche* isomerization is characterized by *FT*i.r. spectroscopy through measurements of the absorbances of characteristically *trans* bands, and characteristically *gauche* bands. *Trans–gauche* isomerization is characterized by ^{13}C n.m.r. spectroscopy through measurements of the ^{13}C chemical shifts in the solid state. *FT*i.r. spectroscopy shows that an increase in temperature results in an increase in the percentage of *gauche* isomers for the methylene units in both the spacer and the mesogen. N.m.r. spectroscopy shows 13% more *gauche* isomers in the high-temperature nematic state, relative to the low-temperature nematic state, for rotation about the C_{28}–C_{29} bond axis in the spacer.

(Keywords: liquid crystalline polymer; isomerization; nematic state)

INTRODUCTION

A new series of liquid crystal polymers (LCPs) has been synthesized, based on the 1-(4-hydroxyphenyl)-2-(2-R-4-hydroxyphenyl)ethane mesogen where R is F, Cl or CH_3[1]. These main-chain LCPs are copolymers with various molar ratios of the R substituents. All of the LCPs in this series have a 33/33/33 molar ratio of flexible spacers containing 5, 7 and 9 methylenic units (see *Scheme 1*). These liquid crystalline copolymers are interesting because several of the LCPs show two nematic states, where the high-temperature nematic state is denoted as n_1, and the low-temperature nematic state as n_2. Of all the LCPs in the series, only F/Cl/M(33/33/33)-5/7/9(33/33/33) does not crystallize[1].

Rotation about the C_7–C_8 axis makes this mesogen relatively flexible. It was hypothesized that the unique properties of these LCPs originate from the use of a 'semi-flexible' mesogen instead of a 'rigid-rod' mesogen[1]. This paper studies the *trans–gauche* isomerization of the methylene groups in the mesogen (C_7 and C_8) and in the spacer (C_{26} through to C_{30}) in order to explain the difference between the two nematic states. Conformational isomerization is characterized by Fourier transform infra-red (*FT*i.r.) spectroscopy and nuclear magnetic resonance (n.m.r.) spectroscopy.

FT*i.r. spectroscopy*

Because of the fast time-scale of the *FT*i.r. experiment (i.e. ps), separate peaks are observed for methylene groups that are in the *trans* and for methylene groups in the *gauche* conformation. *FT*i.r., in fact, produces a 'snapshot' because the *FT*i.r. experiment is on a faster time-scale than the *trans–gauche* rotation[2].

The area of the infra-red peak is proportional to the amount of the particular conformation. If the ratio of the *trans* isomers increases, then the *FT*i.r. peaks assigned to the *trans* conformations will increase in intensity while the peaks assigned to the *gauche* conformations will decrease in intensity[3,4].

However, absorbance alone is not sufficient to deduce the percentage of the respective conformations. According to Beer's law, the absorbance A is equal to the extinction coefficient ε, multiplied by the path length l and the concentration of the absorbing species c:

$$A = \varepsilon l c \tag{1}$$

To determine the percentage of the respective conformations, the absorbance of the *gauche* band is divided by the absorbance of a *trans* band. When the two absorbances are ratioed, the path length is equal for both, and assuming the extinction coefficients are constant, the ratio of the absorbances is proportional to the ratio of the concentrations:

$$\frac{A_g}{A_t} = \frac{\varepsilon_g l c_g}{\varepsilon_t l c_t} \propto \frac{c_g}{c_t} \tag{2}$$

However, this analysis assumes that the extinction coefficients are either constant or independent of temperature. If the absorbance of the band increasing in intensity is plotted *versus* the absorbance of the corresponding decreasing band, a straight line proves that the extinction coefficients are independent of temperature (or,

* To whom correspondence should be addressed

0032-3861/94/12/2528–10

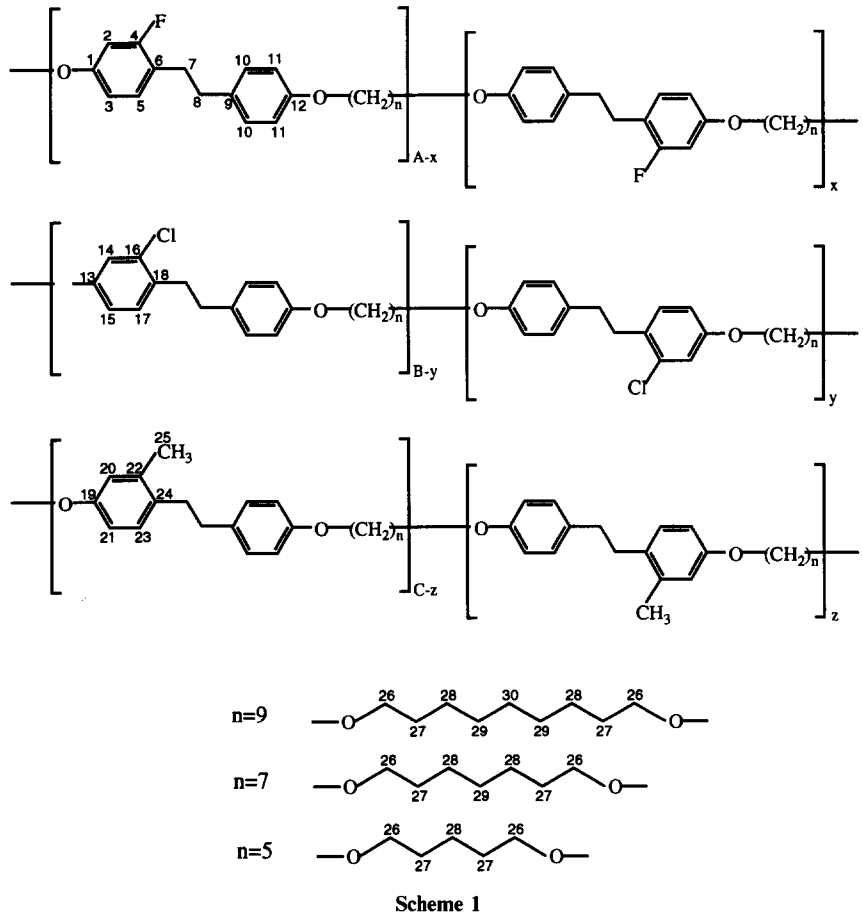

Scheme 1

less likely, that the two bands have the same temperature dependence)[5].

Solid-state ^{13}C n.m.r. spectroscopy

In the solid state, the ^{13}C n.m.r. chemical shifts (δ) are influenced by (A) the intramolecular conformation and (B) the intermolecular packing effects. Therefore, if the intermolecular packing does not change, the chemical shifts can be used to distinguish the conformational isomers.

Conformational or geometric isomers are magnetically inequivalent due to their differing chemical bond angles and differing solid-state environments. This magnetic inequivalence results in inequivalent chemical shifts[6].

The through-space distance between the observed carbon, C_o, and the carbon which is three bonds away, C_γ, changes with rotation between the *trans* and *gauche* isomers. The distance from C_o to C_γ is reduced in the *gauche* conformation. Therefore, in the *gauche* conformation C_o is shielded by C_γ, resulting in an upfield shift of the chemical shift of C_o[7]. A γ-carbon in the *gauche* conformation causes a shielding of -5.2 ppm[8], while two γ-*gauche* carbons, one on each side of C_o, will double the amount of shielding. It should be noted that the chemical shift of C_o is representative of isomerization at the central bond between C_o and C_γ. This phenomenon is called the γ-*gauche* effect[8].

Since rotation between *trans* and *gauche* isomers occurs faster than the time-scale of the n.m.r. experiment, separate peaks are not observed for the two isomers. Instead, there is a single peak whose chemical shift is indicative of the ratio of isomers, i.e. the n.m.r. peak has a chemical shift positioned between where the peak would appear for either an all-*trans*, or for an all-*gauche* conformation. If the ratio of *gauche* isomers increases, the n.m.r. peak position will move upfield to smaller values of chemical shift. Therefore, the chemical shift can be used to calculate the relative amounts of the two conformations by using the following equation:

$$\Delta\delta = nf_g\gamma_{c-x} \tag{3}$$

where $\Delta\delta$ is the change in chemical shift, n is the number of atoms causing shielding, f_g is the fraction in the *gauche* conformation, and γ_{c-x} is the shielding constant (in ppm) caused by the nucleus X.

Conformational isomerization has been studied extensively in polyethylene via changes in the ^{13}C chemical shifts caused by the γ-*gauche* effect[9–13].

EXPERIMENTAL

*FT*i.r. transmission spectra were acquired on a Bio-Rad Digilab FTS-60 spectrometer. A resolution of 4 cm^{-1} was used, and 256 interferograms were co-added for each spectrum. Each of these was then digitally divided by a previously run background. The sample was melted on to KBr plates to achieve a thickness which was within the limits of Beer's law. *FT*i.r. spectra were collected over the temperature range 13–169°C for the first heating, cooling and second heating scans. Once calibrated, the temperature controller was accurate to 3.0°C.

Solid-state n.m.r. spectra were collected on a Bruker MSL-300 spectrometer at a ^{13}C measuring frequency of 75.47 MHz. All spectra were collected using a simple one-pulse Bloch decay sequence (^{13}C 90°–acq.–T_R) with gated high-powered proton decoupling (GHPD) and magic angle spinning (MAS). Rates of 3.0–3.2 kHz were used for magic angle sample spinning. The recycle delay

Table 1 Thermal transitions for the copolymers F/Cl/M(*A*/*B*/*C*)-5/7/9(33/33/33)[1] [a]

Copolymer, (*A*/*B*/*C*) molar ratio	Thermal treatment	Thermal transitions (°C)
100/0/0	1st heating	g 24 k_2 48 k_1 102 n_1 106 i
	2nd heating	g 12 k_1 103 n_1 106 i
	Cooling	g 1 k_1 87 n_1 99 i
0/100/0	1st heating	g 10 k 43 n_2 49 n_1 68 i
	2nd heating	g 9 n_2 49 n_1 68 i
	Cooling	g 3 n_2 44 n_1 60 i
33/33/33	1st heating	g 13 n_2 69 n_1 82 i
	2nd heating	g 11 n_2 69 n_1 82 i
	Cooling	g 5 n_2 63 n_1 74 i

[a] Key to abbreviations: M, CH_3; g, glass; k, crystalline; n_2, low-temperature nematic; n_1, high-temperature nematic; i, isotropic

Table 2 Number-average molecular weight (M_n) and polydispersity (M_w/M_n) for the copolymers F/Cl/M(*A*/*B*/*C*)-5/7/9(33/33/33)[1]

Copolymer, (*A*/*B*/*C*) molar ratio	M_n	M_w/M_n
100/0/0	21 000	2.01
0/100/0	18 600	1.98
33/33/33	28 000	2.34

between pulse sequence repetitions (T_R) was 5 s. This was sufficient to re-establish a Boltzmann equilibrium as the longest T_1 was just over 1 s. Typically, 5000 scans were signal-averaged for each spectrum. However, the number of scans varied from 2000 to 7000 depending on the quantity of sample. All spectra were collected with quadrature phase detection, and the temperature was varied with a temperature controller which was accurate to 0.5°C.

Samples were spun in Zirconia rotors (outer diameter = 7 mm) with Kel-F caps and the magic angle was set by maximizing the ^{79}Br peak intensities of KBr[14]. The radio frequency (r.f.) fields ranged from 35–37 kHz, as calculated from the length of a 90° pulse. The 90° pulse length was determined from null intensities of adamantane at 360° and 720°. Free induction decays (FIDs) with 135 W to 3 K data points, were collected and zero filled to 8 K data points before the Fourier transformation process. The number of data points collected varied widely, because T_2 was extremely short at lower temperatures. The chemical-shift scale was set from the known peak positions of adamantane. Field drift was monitored by checking the chemical-shift scale with adamantane, both before and after the experiments, and was found to be negligible.

After the first heating scan, the sample was ejected from the magnetic field and cooled before the second heating scan. In this manner, the sample was not cooled in the field, nor cooled while spinning. If the sample had been cooled while spinning in the field, nematic orientation would have been locked into place, even at lower temperatures[15].

All of the *FT*i.r. and n.m.r. spectra were transferred via Ethernet to a MicroVax III+ computer for subsequent spectral manipulation using various in-house programs written in Fortran 77.

RESULTS

Previously published differential scanning calorimetry (d.s.c.) and gel permeation chromatography (g.p.c.) data of the LCPs in the study are given in *Tables 1* and *2*, respectively[1]. It should be noted that two nematic states are observed, i.e. n_2, the low-temperature nematic state, and n_1, the high-temperature nematic state. It can also be seen that the F/Cl/M(33/33/33)-5/7/9(33/33/33) copolymer is the only LCP which does not crystallize. Furthermore, the first heating scan differs from the second heating scan for all of the copolymers, with the exception of this material.

FT*i.r. spectroscopy*

*FT*i.r. spectra of all three copolymers are shown in *Figure 1*, with the tentative peak assignments given in *Tables 3–5*. All of the expected bands are observed[16–18], with the peak assignments consistent within the three polymers. Furthermore, the peak assignments for the methylene groups in the spacers agree with those obtained for polyethylene (PE)[19,20], while the peak assignments for the methylene groups in the mesogens agree with those obtained for 1,2-diphenylethane (DPE)[21–23]. The peaks of interest are those assigned to the *trans* and *gauche* modes.

The *FT*i.r. spectra of the copolymer sample F/Cl/M (33/33/33)-5/7/9(33/33/33) show changes in the baseline with temperature, thus making baseline correction necessary. This was carried out separately for each region of interest by subtracting a wedge.

Figure 2 shows the baseline corrected spectra for the first heating scan of copolymer F/Cl/M(33/33/33)-5/7/9 (33/33/33). The peaks at 727 and 758 cm^{-1}, assigned to modes of the *trans* conformation, decrease in intensity, as shown in *Figure 2a*. Correspondingly, the peak at 1440 cm^{-1}, assigned to a *gauche* mode, increases, as shown in *Figure 2b*.

The peak intensities for the first heating, cooling and second heating scans are shown in *Figures 3a–3e* for all of the conformationally sensitive bands. The peak intensities were baseline corrected and then normalized with respect to the absorbance at room temperature. For all of the peaks, as the temperature is increased the *gauche* bands increase in intensity, while the *trans* bands decrease

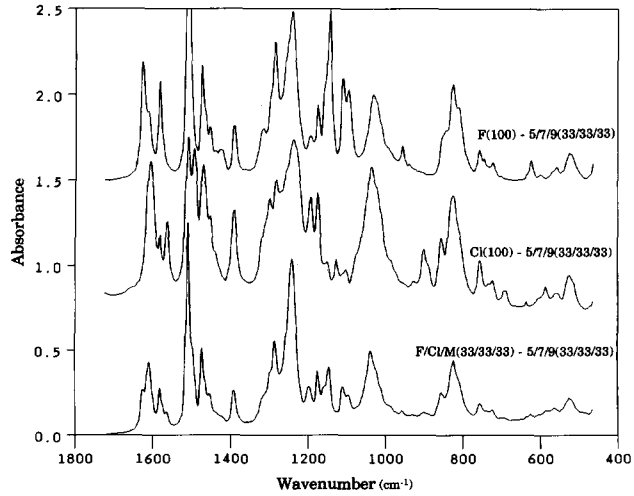

Figure 1 *FT*i.r. spectra of the F(100)-5/7/9(33/33/33), Cl(100)-5/7/9 (33/33/33) and F/Cl/M(33/33/33)-5/7/9(33/33/33) copolymers from 1700 to 450 cm^{-1}

Table 3 *FT*i.r. peak assignments for the F(100)-5/7/9(33/33/33) copolymer

Peak, intensity[a]	Peak assignment[b]
1628s	C–C stretching of 1,2,4 tri sub Ph
1614m,sh	C–C stretching of *para* di sub Ph
1584s	C–C stretching of 1,2,4 tri sub Ph
	Weak C–C stretching of *para* di sub Ph
1510vvs	C–C stretching of 1,2,4 tri sub Ph
	C–C stretching of *para* di sub Ph
1476s	PE *trans* methylene bending (scissoring)
	DPE *trans* methylene bending (scissoring)
1456m	C–C stretching of 1,2,4 tri sub Ph
	C–C stretching of *para* di sub Ph
1443vw	PE *–GG–* methylene bending (scissoring)
1393m	PE *–GTG–* methylene wagging symmetric
1317m	PE *–GTG–* methylene wagging antisymmetric
1287s	PE methylene wagging of $-CH_2-O-$, tentative
1244vs	Ph–O asymmetrical C–O–C stretching
1196m	DPE C–C stretch, tentative
1177m	DPE C–C stretch, tentative
1157m,sh	PE *trans* methylene twist
	DPE *trans* methylene twist
1146vs	Ph–F stretching
1111s	$-CH_2-O-$ asymmetrical C–O–C stretching
1097s	PE C–C stretch
1034s	Ph–O symmetrical C–O–C stretching
	Possible contribution from ring breathing
959m	$-CH_2-O-$ symmetrical C–O–C stretching
	Possible contribution from DPE C–Ph stretch
847m,sh	1,2,4 tri sub Ph C–H out-of-plane deformation
827s	*para* di sub Ph C–H out-of-plane deformation
812m,sh	1,2,4 tri sub Ph C–H out-of-plane deformation
762m	DPE *trans* methylene rocking
727m	PE *trans* methylene rocking

[a] Key to abbreviations for peak intensities: vvs, very very strong; vs, very strong; s, strong; m, medium; w, weak; vw, very weak; vvw, very very weak and sh, shoulder

[b] Key to abbreviations for peak assignments: PE, methylene in polyethylene-like spacer segments; DPE, methylene in 1,2-diphenylethane-like segments; Ph, phenyl and sub, substituted

in intensity. In general, the polymer has a higher *gauche* content at higher temperatures. This is true for the methylene groups, both in the spacer and in the mesogen. The discontinuities at the nematic/isotropic transition will be explained briefly below.

From plots of the absorbance as a function of temperature it is evident that the polymer has more *gauche* character at higher temperatures. However, the absorbance could change, due to (a) mass flow or to (b) a change in the extinction coefficient. According to equation (2) a plot of the ratio of the absorbances will be proportional to the ratio of the concentrations of the isomers.

Most of the methylene peaks are assigned to a particular conformation for both the polyethylene-like spacer segments and the 1,2-diphenylethane-like mesogen segments. However, the peak at 727 cm^{-1} is a *trans* band of only the polyethylene-like segments and the peak at 1440 cm^{-1} is a *gauche* band of only the polyethylene-like segments. Using these two peaks assigned to only polyethylene-like segments, the ratio of the *gauche* (1440 cm^{-1}) to *trans* (727 cm^{-1}) absorbance is plotted as a function of temperature in *Figure 4a*. According to equation (2), this shows clearly the increase in the concentration of *gauche* isomers, relative to that of *trans* isomers.

Any mass flow causing a change in absorbance is normalized by ratioing the two absorbances. Also, it is unlikely that mass flow occurs, since after cooling the absorbance returns to its initial value.

Recall however that ratioing the two absorbances (equation (2)) assumes that the extinction coefficients are constant with temperature. If the absorbance of the increasing band is plotted *versus* the absorbance of the corresponding decreasing band, a straight line proves that the extinction coefficients are independent of temperature[5]. *Figure 4b* plots the absorbance of the 1440 cm^{-1} band *versus* the 727 cm^{-1} band, showing that the extinction coefficients are not constant. The plot displays two relatively parallel lines with a discontinuity at the nematic/isotropic transition. Therefore, the extinction coefficients are constant throughout the glass (g), n_2 and n_1 states, and constant again in the isotropic (i) state. However, the extinction coefficients change at the n_1 to i transition, which explains the discontinuities in *Figures 3a–3e*. It seems most likely that the change in the extinction coefficient is caused by a change in intermolecular interaction, as a result of a change in density. Indeed, X-ray scattering patterns of this polymer show a discontinuous increase in the average distance between chains of 0.051 Å at the n_1 to i transition[1].

The *FT*i.r. data show a general trend towards an increased percentage of *gauche* isomers with heating for the methylene units in both the spacer and the mesogen. However, the *FT*i.r. data are not sufficient to explain the difference between the two nematic states.

Table 4 *FT*i.r. peak assignments for the Cl(100)-5/7/9(33/33/33) copolymer

Peak, intensity[a]	Peak assignment[b]
1609s	C–C stretching of 1,2,4 tri sub Ph
	C–C stretching of *para* di sub Ph
1584m	C–C stretching of *para* di sub Ph
1564s	C–C stretching of 1,2,4 tri sub Ph
1512s	C–C stretching of *para* di sub Ph
1497s	C–C stretching of 1,2,4 tri sub Ph
1474	PE *trans* methylene bending (scissoring)
	DPE *trans* methylene bending (scissoring)
1454m	C–C stretching of 1,2,4 tri sub Ph
	C–C stretching of *para* di sub Ph
1441vw,sh	PE *–GG–* methylene bending (scissoring)
1393s	PE *–GTG–* methylene wagging symmetric
1316vw,sh	PE *–GTG–* methylene wagging antisymmetric
1300m	?
1285s	PE methylene wagging of $-CH_2-O-$, tentative
1240s	Ph–O asymmetrical C–O–C stretching
1194s	DPE C–C stretch, tentative
1177s	DPE C–C stretch, tentative
1152w	PE *trans* methylene twist
	DPE *trans* methylene twist
1128m	$-CH_2-O-$ asymmetrical C–O–C stretching
1103w	Ph–Cl stretching
1040s	Ph–O symmetrical C–O–C stretching
930w	$-CH_2-O-$ symmetrical C–O–C stretching
	DPE C–Ph stretch
902m	?
856m	1,2,4 tri sub Ph C–H out-of-plane deformation
826s	*para* di sub Ph C–H out-of-plane deformation
810w,sh	1,2,4 tri sub Ph C–H out-of-plane deformation
758m	DPE *trans* methylene rocking
727w	PE *trans* methylene rocking

[a] Key to abbreviations for peak intensities: vvs, very very strong; vs, very strong; s, strong; m, medium; w, weak; vw, very weak; vvw, very very weak and sh, shoulder

[b] Key to abbreviations for peak assignments: PE, methylene in polyethylene-like spacer segments; DPE, methylene in 1,2-diphenylethane-like segments; Ph, phenyl and sub, substituted

Table 5 *FT*i.r. peak assignments for the F/Cl/M(33/33/33)-5/7/9(33/33/33) copolymer

Peak, intensity[a]	Peak assignment[b]
1626w	C–C stretching of Ph
1611s	C–C stretching of Ph
1584m	C–C stretching of Ph
1566w	C–C stretching of Ph
1512vs	C–C stretching of Ph
1499w,sh	C–C stretching of Ph
1476s	PE *trans* methylene bending (scissoring) DPE *trans* methylene bending (scissoring)
1460vw,sh	$-CH_3$ bending deformation asymmetrical
1456w	C–C stretching of Ph
1440vvw	PE *–GG–* methylene bending (scissoring)
1393m	PE *–GTG–* methylene wagging symmetric
1380vw,sh	$-CH_3$ bending deformation symmetrical
1315w,sh	PE *–GTG–* methylene wagging antisymmetric
1298w,sh	?
1287s	PE methylene wagging of $-CH_2-O-$, tentative
1244vs	Ph–O asymmetrical C–O–C stretching
1198m	DPE C–C stretch, tentative
1177m	DPE C–C stretch, tentative
1159w,sh	PE *trans* methylene twist DPE *trans* methylene twist
1148m	Ph–F stretching
1111m	$-CH_2-O-$ asymmetrical C–O–C stretching Possible contribution from Ph–Cl stretch
1097w	PE C–C stretch Possible contribution from Ph–Cl stretch
1040s	Ph–O symmetrical C–O–C stretching
1026w,sh	Ring breathing
1013w,sh	DPE C–Ph stretch
959w	$-CH_2-O-$ symmetrical C–O–C stretching
903w	?
856m	1,2,4 tri sub Ph C–H out-of-plane deformation
826s	*para* di sub Ph C–H out-of-plane deformation
810w,sh	1,2,4, tri sub Ph C–H out-of-plane deformation
758m	DPE trans methylene rocking
727w	PE *trans* methylene rocking

[a] Key to abbreviations for peak intensities: vvs, very very strong; vs, very strong; s, strong; m, medium; w, weak; vw, very weak; vvw, very very weak and sh, shoulder

[b] Key to abbreviations for peak assignments: PE, methylene in polyethylene-like spacer segments; DPE, methylene in 1,2-diphenylethane-like segments; Ph, phenyl and sub, substituted

N.m.r. spectroscopy and intramolecular conformation

Solid-state ^{13}C n.m.r. spectra for all three copolymers are shown in *Figures 5a–5c*. A decrease in linewidth (i.e. an increase in T_2) with increased temperature can be seen. The n.m.r. peak assignments are given in *Tables 6–8*, where the carbon atoms correspond to those labelled in the chemical formulae of *Scheme 1*. Peak assignments were made by combining information obtained from the following: (a) chemical shift calculations accounting for substituent effects[18,24], (b) quantitative n.m.r. peak areas, (c) comparison to known chemical shifts of model compounds with analogous structures[18], (d) spectral editing of pulse sequences, and (e) comparison of the various spectra in this analogous series with each other. The n.m.r. peak assignments are in agreement with peak assignments previously published for similar LCPs[25,26].

Tables 6–8 also list the solid-state chemical shifts in the various states. N.m.r. spectra were neither smoothed or baseline corrected before the peak positions were determined. Either of these operations might have artificially shifted the peak positions. However, the spectra in *Figures 5* and *6* were baseline corrected for presentation purposes. The baseline correction algorithm uses piecewise polynomial functions to connect the user-defined zero positions. The aliphatic regions of the spectra are shown expanded in *Figures 6a–6c* for the first heating scans.

Figure 6a shows the aliphatic region of the spectra of the F(100)-5/7/9(33/33/33) copolymer in the g (29°C), k_2 (45°C), k_1 (67°C) and n_1 (97°C) states. It should be noted that the chemical shift of C_{27} shifts upfield at the transition from the k_1 state to the n_1 state, showing that the latter state has more *gauche* character.

Figure 6b shows the aliphatic region of the spectra of the Cl(100)-5/7/9(33/33/33) copolymer in the g (30°C), k (40°C), n_2 (44°C), n_1 (55°C) and i (75°C) states. In this case, it is found that the chemical shift of C_{27} shifts upfield at the transition from the n_1 state to the i state, showing that the i state has more *gauche* character.

Figure 6c shows the aliphatic region of the spectra of the F/Cl/M(33/33/33)-5/7/9(33/33/33) copolymer in the g (27°C), n_2 (62°C), n_1 (72°C), and i (86°C) states. Here, it is noted that the chemical shift of C_{27} shifts upfield at the transition from the n_2 state to the n_1 state, showing that the latter state has more *gauche* character. We believe that the reason for the F/Cl/M(33/33/33)-5/7/9(33/33/33) copolymer having different mesomorphic properties to

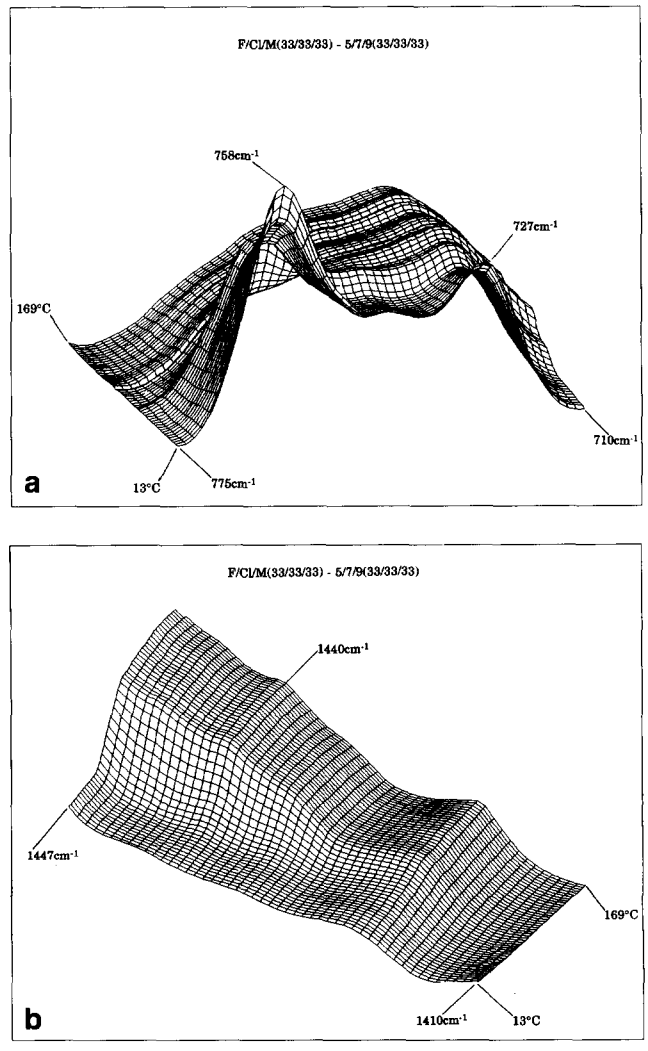

Figure 2 *FT*i.r. spectra of the F/Cl/M(33/33/33)-5/7/9(33/33/33) copolymer from 13 to 169°C for: (a) the DPE *trans* methylene rocking peak at 758 cm^{-1} and the PE *trans* methylene rocking peak at 727 cm^{-1} and (b) the PE *–GG–* methylene bending (scissoring) peak at 1440 cm^{-1}

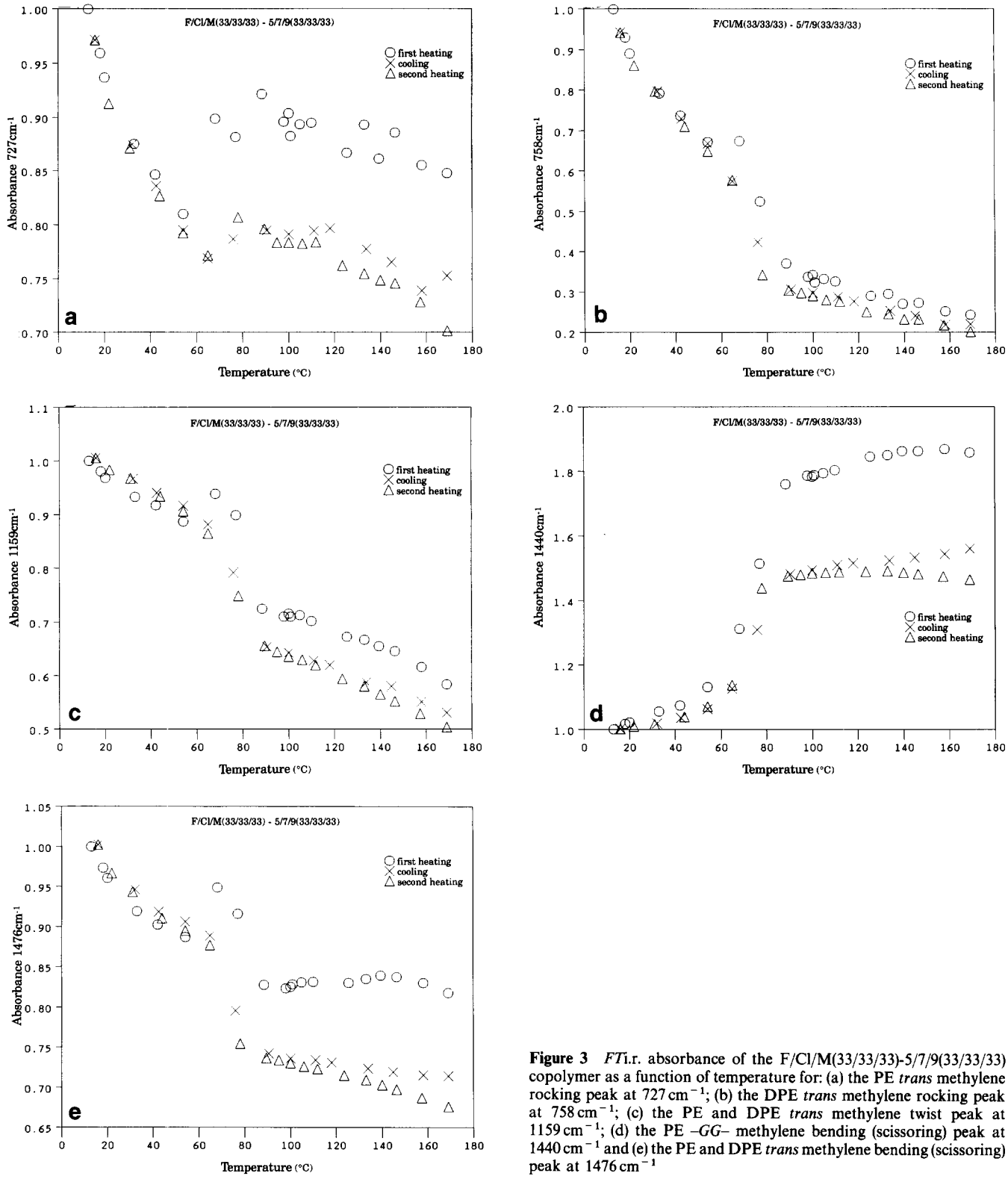

Figure 3 *FT*i.r. absorbance of the F/Cl/M(33/33/33)-5/7/9(33/33/33) copolymer as a function of temperature for: (a) the PE *trans* methylene rocking peak at 727 cm^{-1}; (b) the DPE *trans* methylene rocking peak at 758 cm^{-1}; (c) the PE and DPE *trans* methylene twist peak at 1159 cm^{-1}; (d) the PE *–GG–* methylene bending (scissoring) peak at 1440 cm^{-1} and (e) the PE and DPE *trans* methylene bending (scissoring) peak at 1476 cm^{-1}

the other polymers (i.e. lack of crystallization, lack of thermal history) is because isomerization occurs between the two nematic states.

In all cases, it is the chemical shift of C_{27} that changes. C_{27} has two γ-substituents, namely a γ-phenyl in the direction of the mesogen, and a γ-methylene in the direction of the spacer. It is reasonable to assume that the γ-phenyl group is all-*trans* due to the steric bulkiness of the phenyl group. Therefore, a change in the chemical shift of C_{27} is due to rotation about the bond axis between C_{28} and C_{29}.

The change in the chemical shift can be used to calculate the fraction of methylene groups that change conformation, according to equation (3). For the copolymer F/Cl/M(33/33/33)-5/7/9(33/33/33) the chemical shift changes from 30.6 ppm for n_2 to 29.9 ppm for n_1. Therefore, $\Delta\delta = 29.9\text{ ppm} - 30.6\text{ ppm} = -0.7\text{ ppm}$. Since it is assumed that the γ-phenyl group is exclusively *trans*, only the γ-methylene group causes a shielding in the *gauche* conformation so that $n = 1$. The shielding caused by a γ-methylene group is $\gamma_{c-c} = -5.2$ ppm. Therefore, by solving equation (3), $f_g = 0.13$, i.e. the high-temperature

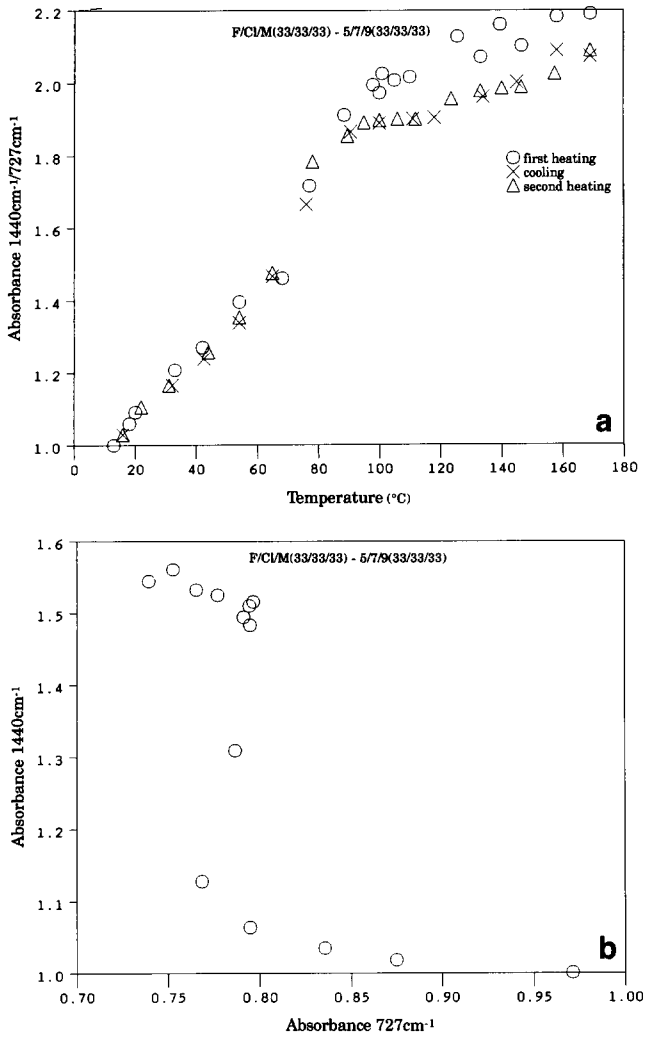

Figure 4 (a) *FT*i.r. absorbance of the peak at 1440 cm^{-1} ratioed to the peak at 727 cm^{-1} as a function of temperature for the F/Cl/M (33/33/33)-5/7/9(33/33/33) copolymer. (b) Plot of the absorbance of the peak at 1440 cm^{-1} *versus* the absorbance of the peak at 727 cm^{-1} for the F/Cl/M(33/33/33)-5/7/9(33/33/33) copolymer

nematic state, n_1, has 13% more *gauche* isomers than the low-temperature nematic state, n_2. In conclusion, the difference between the two nematic states is 13% more *gauche* isomers in the high-temperature nematic state for the bond between C_{28} and C_{29}.

The chemical shifts measured for the second heating scan are almost the same as those obtained for the first scan. Therefore, conformational isomerization does not explain the presence or absence of hysteresis.

Analogous LCPs, containing only methyl substituents on the phenyl ring, and spacers of five and nine methylene units have previously been studied by Cheng *et al.*[26]. Similarly, changes in ^{13}C chemical shifts were interpreted in terms of the *γ-gauche* effect. For these polymers also, there is a larger fraction of *gauche* isomers in the spacer at higher temperatures[26].

N.m.r. spectroscopy and intermolecular packing

In addition to C_{27}, the chemical shifts of several other carbons change in the various states. To study the rotation about the C_7–C_8 axis, changes in the chemical shifts of C_6, C_9, C_{18} and C_{24} need to be determined. However, changes in the chemical shifts cannot always be interpreted solely in terms of the intramolecular conformation. Intermolecular packing also affects the solid-state ^{13}C chemical shift. At lower temperatures there is tighter intermolecular packing, which results in increased shielding, thereby causing a lower chemical shift. For several of the carbons, the chemical shifts change as a result of both conformational and packing effects.

When a mixture of these effects (conformation and packing) shifts the chemical shifts, the chemical shift

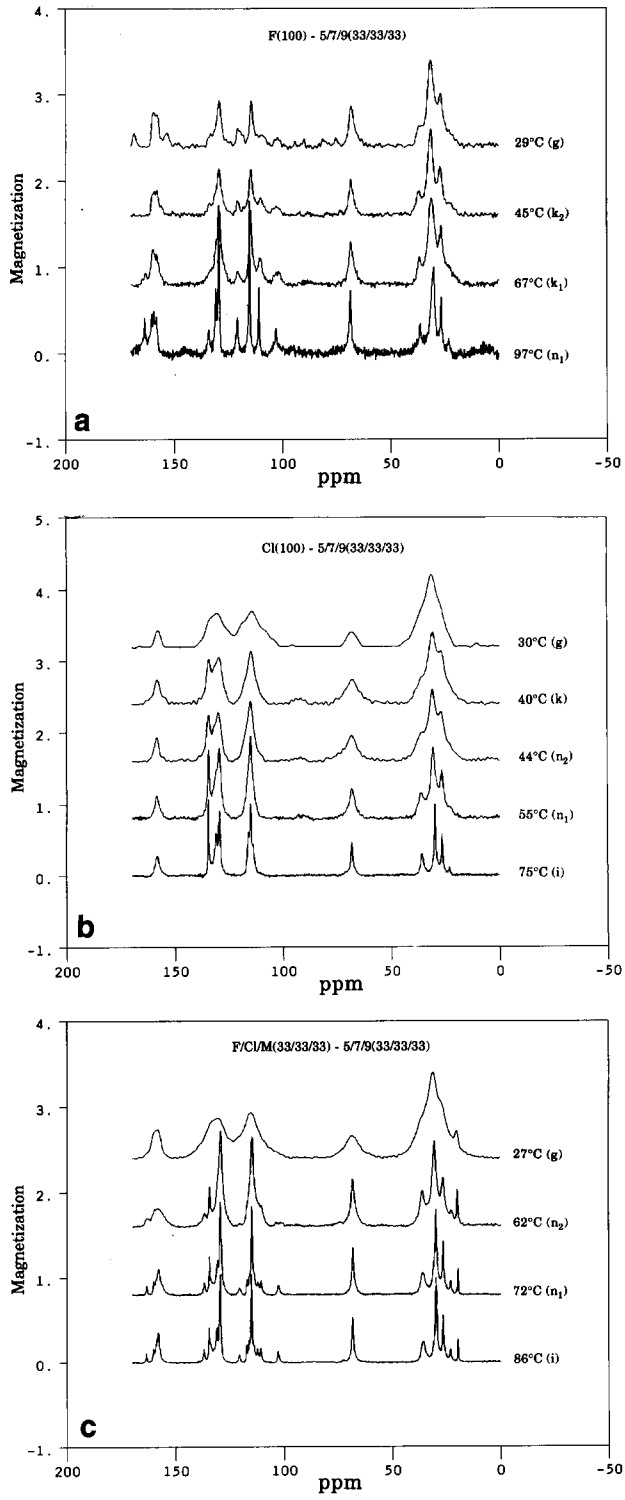

Figure 5 Solid-state ^{13}C n.m.r. spectra for the first heating scan of: (a) the F(100)-5/7/9(33/33/33) copolymer at 29, 45, 67 and 97°C; (b) the Cl(100)-5/7/9(33/33/33) copolymer at 30, 40, 44, 55 and 75°C and (c) the F/Cl/M(33/33/33)-5/7/9(33/33/33) copolymer at 27, 62, 72 and 86°C

Table 6 ^{13}C n.m.r. chemical shifts of the F(100)-5/7/9(33/33/33) copolymer

	δ(ppm)			
Assignment	29°C g	45°C k_2	67°C k_1	97°C n_1
First heating				
C_4	168.5	163.9	163.3	163.7
C_1	159.4	159.6	159.8	159.5
C_{12}	157.7	158.0	158.1	158.3
C_9	133.1	133.6	133.5	134.1
C_5	–	131.0	130.9	130.9
C_{10}	129.3	129.3	129.3	129.5
C_6	120.7	120.9	120.9	120.9
C_{11}	114.4	114.6	114.8	115.3
C_3	109.9	110.0	110.4	110.9
C_2	102.4	102.9	102.7	103.0
C_{26}	68.3	68.4	68.5	68.7
C_7, C_8	36.7	36.7	36.7	36.3
C_{27}	31.3	31.3	31.0	30.0
C_{29}, C_{30}	26.8	27.0	26.6	26.5
C_{28}	22.8	22.2	22.3	23.0
Assignment	29°C g	45°C k_2	67°C k_1	95°C n_1
Second heating				
C_4	–	–	163.6	163.7
C_1	159.5	159.7	160.0	160.4
C_{12}	158.3	157.9	157.5	158.4
C_9	134.1	134.1	–	133.9
C_5	131.2	130.8	–	130.9
C_{10}	129.7	129.6	129.3	129.5
C_6	120.7	120.9	120.6	121.0
C_{11}	114.7	114.8	114.6	115.3
C_3	110.3	109.9	110.6	111.0
C_2	103.5	102.7	103.1	102.7
C_{26}	68.6	68.4	68.4	68.7
C_7, C_8	36.7	36.9	36.9	36.6
C_{27}	31.6	31.6	31.3	30.5
C_{29}, C_{30}	27.4	27.2	26.5	26.6
C_{28}	23.0	22.7	23.2	22.9

becomes difficult to interpret, e.g. the chemical shift of C_9 cannot be interpreted solely on the basis of the *γ-gauche* effect. Conformational isomerization about the C_7–C_8 axis also changes the intermolecular packing, which therefore affects the chemical shift. Packing effects are particularly relevant in this case due to the bulkiness of the phenyl group.

It was hoped to determine the conformation about the C_7–C_8 axis from the ^{13}C chemical shifts of the C_6, C_9, C_{18} and C_{24} atoms. However, the chemical shifts of all of the aromatic carbons are dominated by packing effects. Nearly all of the aromatic chemical shifts move to higher ppm values at higher temperatures. Therefore, *trans–gauche* isomerization may occur about the C_7–C_8 bond axis in the mesogen, but this cannot be determined from the ^{13}C chemical shifts.

For similar LCPs, Cheng *et al.*[26] observed changes in the solid-state chemical shifts of C_7 and C_8. These workers also concluded that changes in the chemical shifts of these carbons cannot be interpreted in terms of the *γ-gauche* effect, due to the fact that the alkyl chain (ethylene) is not sufficiently long. For short alkyl chains, intermolecular packing effects dominate the ^{13}C chemical shifts[26].

DISCUSSION

Molecular packing

At lower temperatures the flexible alkyl spacer has a larger percentage of *trans* isomers. At higher temperatures the spacer is more *gauche* in character, or more coiled. *Trans* isomers are capable of packing regularly in a crystalline or liquid crystalline lattice[27,28]. Upon cooling from the isotropic state to the nematic state, the LCP becomes liquid crystalline when the spacer has enough *trans* character to allow regular packing in a liquid crystalline lattice[29]. Upon further cooling, the LCP crystallizes if the spacer acquires enough additional *trans* character to allow a more regular packing. This is in complete analogy to polyethylene, where crystalline material is all-*trans*.

Of the six LCPs that have been synthesized in this series, only the F/Cl/M(33/33/33)-5/7/9(33/33/33) copolymer does not crystallize. All of the *A/B/C*(100/0/0)-5/7/9 (33/33/33) and *A/B/C*(50/50/0)-5/7/9(33/33/33) materials crystallize. In the case of the former LCPs, all of the phenyl rings have the same substituent. These copolymers crystallize because the polymer repeat-units all have the same substituent and are therefore capable of packing in a regular manner. However, in the latter case the LCPs contain two different types of substituents, but there is still not enough heterogeneity to perturb the regular packing and these copolymers do, in fact, crystallize. Finally, in the case of the F/Cl/M(33/33/33)-5/7/9(33/33/33) copolymer there are three different types of substituents, and their presence causes enough heterogeneity in the packing that this LCP does not crystallize. Due to the

Table 7 ^{13}C n.m.r. chemical shifts of the Cl(100)-5/7/9(33/33/33) copolymer

	δ(ppm)				
Assignment	30°C g	40°C k	44°C n_2	55°C n_1	75°C i
First heating					
C_{12}, C_{13}	157.6	158.1	158.3	158.5	158.3
C_9, C_{16}, C_{18}	134.0	134.4	134.5	134.6	134.6
C_{17}	–	131.6	131.7	130.9	131.3
C_{10}	130.4	129.8	130.0	129.7	129.7
C_{14}	–	–	117.1	116.2	116.3
C_{11}	114.5	114.9	115.2	115.1	115.2
C_{15}	–	–	113.4	113.9	114.2
C_{26}	68.8	68.2	68.6	68.6	68.5
C_7, C_8	35.8	35.9	35.6	36.2	35.7
C_{27}	31.3	30.8	30.9	30.7	30.0
C_{29}, C_{30}	27.1	26.8	27.0	26.7	26.6
C_{28}	22.9	22.4	23.0	22.8	23.2
Assignment	30°C g	42°C n_2	55°C n_1		75°C i
Second heating					
C_{12}, C_{13}	157.5	158.5	158.3		158.3
C_9, C_{16}, C_{18}	133.9	134.4	134.4		134.6
C_{17}	–	130.8	131.1		131.2
C_{10}	129.6	129.7	129.6		129.7
C_{14}	117.1	116.8	116.5		116.3
C_{11}	114.8	115.0	115.0		115.2
C_{15}	–	–	113.4		113.9
C_{26}	67.7	68.4	68.5		68.5
C_7, C_8	36.9	36.2	–		35.7
C_{27}	30.3	30.5	30.5		29.9
C_{29}, C_{30}	26.9	26.8	26.7		26.5
C_{28}	–	–	–		23.2

Table 8 ^{13}C n.m.r. chemical shifts of the F/Cl/M(33/33/33)-5/7/9 (33/33/33) copolymer

	δ(ppm)			
Assignment	27°C g	62°C n_2	72°C n_1	86°C i
First heating				
C_4	163.4	163.0	163.5	163.6
C_1	160.0	159.8	160.3	160.3
C_{12}, C_{13}, C_{19}	158.4	158.3	158.0	158.1
C_{22}	139.3	–	139.1	139.1
C_{24}	–	137.0	137.0	137.0
C_9, C_{16}, C_{18}	133.7	134.4	134.6	134.6
C_5, C_{17}	–	130.8	130.9	131.1
C_{10}, C_{23}	130.4	129.3	129.5	129.5
C_6	121.1	120.7	120.7	120.6
C_{20}	–	117.1	117.2	117.4
C_{14}	–	–	116.1	116.3
C_{11}	115.5	114.9	115.1	115.2
C_{15}	–	–	113.9	114.0
C_{21}	112.1	112.0	112.3	112.4
C_3	109.2	110.7	110.8	110.9
C_2	103.3	102.9	102.7	102.9
C_{26}	68.8	68.3	68.4	68.4
C_7, C_8	36.9	36.1	36.0	35.8
C_{27}	31.3	30.6	29.9	29.8
C_{29}, C_{30}	27.5	26.6	26.5	26.5
C_{28}	–	22.8	23.1	23.2
C_{25}	20.3	19.9	19.7	19.7
Assignment	30°C g	62°C n_2	72°C n_1	86°C i
Second heating				
C_4	–	163.4	163.6	163.7
C_1	–	159.7	159.9	160.4
C_{12}, C_{13}, C_{19}	158.5	158.0	158.1	158.3
C_{22}	–	–	139.1	–
C_{24}	–	137.1	137.1	137.1
C_9, C_{16}, C_{18}	–	134.5	134.6	134.6
C_5, C_{17}	–	131.0	130.9	131.1
C_{10}, C_{23}	130.1	129.4	129.5	129.7
C_6	120.4	120.9	120.9	120.7
C_{20}	–	117.4	117.2	117.4
C_{14}	–	–	116.2	116.3
C_{11}	114.6	115.0	115.1	115.2
C_{15}	–	–	–	–
C_{21}	–	112.1	112.2	112.4
C_3	–	110.8	110.7	111.0
C_2	102.9	102.8	102.8	102.9
C_{26}	68.4	68.4	68.5	68.5
C_7, C_8	37.2	36.3	36.3	35.6
C_{27}	30.1	30.7	30.5	29.9
C_{29}, C_{30}	26.5	26.7	26.7	26.5
C_{28}	–	22.7	23.0	23.2
C_{25}	20.5	20.1	20.0	19.7

varying sizes of the three different pendent groups, the LCP cannot pack in a regular manner and therefore crystallization does not occur.

Error

An estimate was made of the error in ^{13}C chemical shift measurements caused by magnetic field drift. The frequencies of the adamantane resonances were determined before the LCP spectra were collected, and again six days after these spectra were obtained. There was no measurable change found in the frequencies of the adamantane resonances.

An estimate was also made of the total error in ^{13}C chemical shift measurements. The chemical shifts were determined twice for a given sample at a given temperature. Since the two spectra were collected with an intervening time interval of one month, the chemical-shift scale was set each time from the known chemical shifts of adamantane. Many of the chemical shifts are identical. However, some of the chemical shifts differ by ±0.032 ppm. Since the spectral width is 20000 Hz or 265.006 ppm, and the FIDs are Fourier transformed into spectra with 8 K or 8192 W data points, there is a data point every 0.032 ppm. Therefore, the chemical shift measurements are accurate to one data point, i.e. accurate

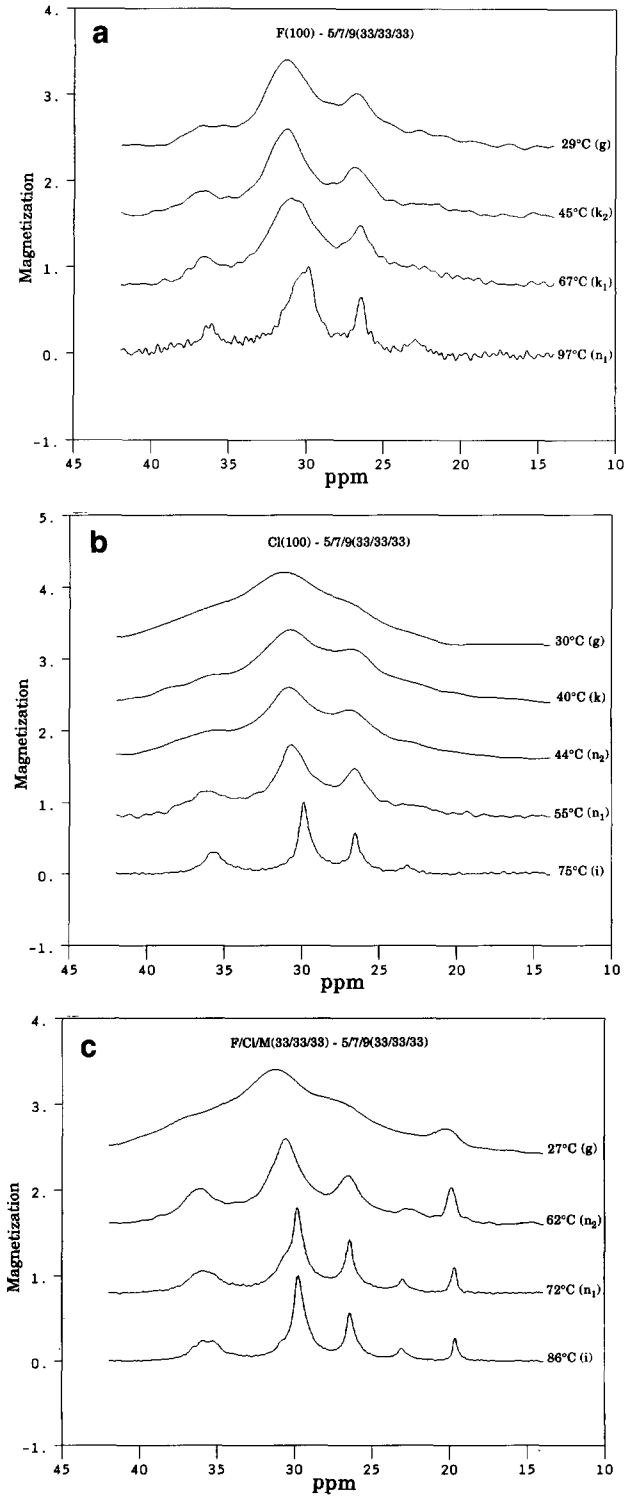

Figure 6 Aliphatic regions of the solid-state ^{13}C n.m.r. spectra for the first heating scan of: (a) the F(100)-5/7/9(33/33/33) copolymer at 29, 45, 67 and 97°C; (b) the Cl(100)-5/7/9(33/33/33) copolymer at 30, 40, 44, 55 and 75°C and; (c) the F/Cl/M(33/33/33)-5/7/9(33/33/33) copolymer at 27, 62, 72 and 86°C

to the limit of the digital resolution. An uncertainty in δ of ± 0.032 ppm propagates via equation (3) to an uncertainty in f_g of ± 0.006 ($\pm 0.6\%$).

CONCLUSIONS

Trans–gauche isomerization is characterized by *FT*i.r. spectroscopy through measurements of the absorbances of bands assigned to modes of the *trans* conformation and those assigned to modes of the *gauche* conformation. In the case of the F/Cl/M(33/33/33)-5/7/9(33/33/33) copolymer, as the temperature is increased, *gauche* bands increase in intensity and *trans* bands decrease in intensity. Therefore, the polymer has more *gauche* character at higher temperatures. This is true for methylene groups both in the spacer and in the mesogen.

Using the two peaks assigned to only polyethylene-like segments in the spacer, the ratio of the absorbance of the *gauche* band (1440 cm^{-1}) to the *trans* band (727 cm^{-1}) is plotted as a function of temperature. This shows an increase in the concentration of *gauche* isomers at higher temperatures.

The absorbance of the increasing band (1440 cm^{-1}) plotted *versus* the absorbance of the corresponding decreasing band (727 cm^{-1}) shows that the extinction coefficients change at the n_1 to i transition. It is most likely that this change in the extinction coefficient is caused by a change in intermolecular spacing.

Trans–gauche isomerization is also characterized by n.m.r. spectroscopy through measurements of the ^{13}C chemical shifts in the solid state. For all three of the copolymers, the chemical shift of C_{27} shifts upfield at higher temperatures, indicating more *gauche* character. A change in the chemical shift of C_{27} is indicative of rotation about the C_{28}–C_{29} bond axis.

In the case of the F/Cl/M(33/33/33)-5/7/9(33/33/33) copolymer the chemical shift of C_{27} shifts -0.7 ppm from the low-temperature nematic state, n_2, to the high-temperature nematic state, n_1. This indicates that the high-temperature nematic state has 13% more *gauche* isomers than the low-temperature nematic state, with respect to rotation about the C_{28}–C_{29} axis in the spacer.

In addition to C_{27}, the chemical shifts of several other carbons change in the various states. However, many of these shifts are dominated by packing effects. Therefore, the chemical shifts cannot be interpreted solely in terms of the γ-*gauche* effect and the intramolecular conformation.

ACKNOWLEDGEMENTS

Special acknowledgement is given to Professor Virgil Percec and Dr Mohammad Zuber from the Department of Macromolecular Science, Case Western Reserve University, for supplying the liquid crystalline copolymers. Also, acknowledgement is given to Professor Bernhard Wunderlich from the Department of Chemistry, University of Tennessee, for supplying preprints of studies of similar polymers. Funding was provided by the Materials Research Group and the National Science Foundation.

REFERENCES

1 Ungar, G., Percec, V. and Zuber, M. *Macromolecules* 1992, **25**, 75
2 Koenig, J. L. 'Spectroscopy of Polymers', American Chemical Society, Washington, DC, 1992
3 Koenig, J. L. and Antoon, M. K. *J. Polym. Sci. Polym. Phys. Edn* 1977, **15**, 1379
4 Lin, S. B. and Koenig, J. L. *J. Polym. Sci. Polym. Phys. Edn* 1982, **20**, 2277
5 O'Reilly, J. M. and Mosher, R. A. *Macromolecules* 1981, **14**, 602
6 Silvestri, R. L. and Koenig, J. L. *Anal. Chim. Acta* 1993, **283**, 997
7 Grant, D. M. and Cheney, B. V. *J. Am. Chem. Soc.* 1967, **89**, 5315
8 Tonelli, A. E. 'NMR Spectroscopy and Polymer Microstructure: The Conformational Connection', VCH, New York, 1989
9 Earl, W. L. and VanderHart, D. L. *Macromolecules* 1979, **12**, 762
10 Ando, I., Yamanobe, T., Sorita, T., Komoto, T., Sato, H., Deguchi, K. and Imanari, M. *Macromolecules* 1984, **17**, 1955
11 Akiyama, S., Komoto, T. and Ando, I. *J. Polym. Sci. Polym. Phys.* 1990, **28**, 587
12 Ando, I., Yamanobe, T. and Asakura, T. *Prog. Nucl. Magn. Reson. Spectrosc.* 1990, **22**, 349
13 Laupretre, F. *Prog. Polym. Sci.* 1990, **15**, 425
14 Frye, J. S. and Maciel, G. E. *J. Magn. Reson.* 1982, **48**, 125
15 Fung, B. M. and Gangoda, M. *J. Chem. Phys.* 1985, **83**, 3285
16 Avram, M. and Mateescu, G. D. 'Infrared Spectroscopy', Robert E. Krieger, New York, 1978
17 'Atlas of Spectral Data and Physical Constants for Organic Compounds' (Eds J. G. Grasselli and W. M. Ritchey), Vol. I, 2nd Edn, CRC Press, Cleveland, OH, 1973
18 Silverstein, R. M., Bassler, G. C. and Morrill, T. C. 'Spectrometric Identification of Organic Compounds', 5th Edn, Wiley, New York, 1991
19 Snyder, R. G. *J. Chem. Phys.* 1967, **47**, 1316
20 Painter, P. C., Coleman, M. M. and Koenig, J. L. 'The Theory of Vibrational Spectroscopy and its Application to Polymeric Materials', Wiley, New York, 1982
21 North, A. M., Pethrick, R. A. and Wilson, A. D. *Spectrochim. Acta Part A* 1974, **30**, 1317
22 Mathur, M. S. and Weir, N. A. *J. Mol. Struct.* 1972, **14**, 303
23 Chiu, K. K., Huang, H. H. and Chia, L. H. L. *J. Chem. Soc. Perkin Trans. 2* 1972, 286
24 Breitmaier, E. and Bauer, G. '^{13}C Nuclear Magnetic Resonance Spectroscopy: A Working Manual', Harwood, New York, 1984
25 Yandrasits, M. A., Cheng, S. Z. D., Zhang, A., Cheng, J., Wunderlich, B. and Percec, V. *Macromolecules* 1992, **25**, 2112
26 Cheng, J., Jin, Y., Wunderlich, B., Cheng, S. Z. D., Yandrasits, M. A., Zhang, A. and Percec, V., unpublished results
27 Yoon, D. Y. and Bruckner, S. *Macromolecules* 1985, **18**, 651
28 Abe, A. and Furuya, H. *Macromolecules* 1989, **22**, 2982
29 Bruckner, S., Scott, J. C., Yoon, D. Y. and Griffin, A. C. *Macromolecules* 1985, **18**, 2709